Micro Gas Turbine Range Extender Performance Analysis Using Varying Intake Temperature

Bin Raja Ahsan Shah, R. M., Al Qubeissi, M., McGordon, A., Amor-Segan, M. & Jennings, P.

Original citation & hyperlink:
Bin Raja Ahsan Shah, RM, Al Qubeissi, M, McGordon, A, Amor-Segan, M & Jennings, P 2020, 'Micro Gas Turbine Range Extender Performance Analysis Using Varying Intake Temperature', *Automotive Innovation*, vol. 3, no. 4, pp. 356-365.
https://doi.org/10.1007/s42154-020-00119-9

DOI 10.1007/s42154-020-00119-9
ISSN 2522-8765
ESSN 2096-4250

Publisher: Springer

The final publication is available at Springer via http://dx.doi.org/10.1007/s42154-020-00119-9

MICRO GAS TURBINE RANGE EXTENDER PERFORMANCE ANALYSIS USING VARYING INTAKE TEMPERATURE

R.M.R.A.Shah[1*], M.A. Qubeissi[1], A.McGordon[2], M.Amor-Segan[2], P.Jennings[2]

[1] Faculty of Engineering, Environment and Computing, Coventry University, CV1 2JH, United Kingdom
[2] Warwick Manufacturing Group, University of Warwick, Coventry, CV4 7AL, United Kingdom

*Corresponding author e-mail and contact number: ac9217@coventry.ac.uk and 00 44 2477 658299

Acknowledgments

The authors would like to thank Technology Strategy Board for providing the funds and support for this research project (TSB Project No: 400224). The authors would also like to thank the project partners, Jaguar Land Rover and Bladon Jets Ltd for providing technical support. Finally, a special thanks to all Vehicle Engineering Facilities technicians at University of Warwick for their assistance in performing the tests.

MICRO GAS TURBINE RANGE EXTENDER PERFORMANCE ANALYSIS USING VARYING INTAKE TEMPERATURE

Abstract

A Micro Gas Turbine can potentially be an alternative power source to the conventional internal combustion engine as a range extender in Hybrid Electric Vehicles. The integration of the Micro Gas Turbine into an automotive vehicle needs a new approach for technical validation requirements compared to the testing of an internal combustion engine. Several attributes of the Micro Gas Turbine are predicted to cause concerns for vehicle sub-system requirements such as high ambient temperature performance and start stop behaviour. This paper describes results from specially developed experimental techniques for testing the Micro Gas Turbine in a typical automotive environment. A black box Micro Gas Turbine was used in this study for performances investigation during hot and cold starts. The Micro Gas Turbine was instrumented and fitted with automotive standard components to replicate typical vehicle operational conditions. The intake air temperature was varied between 10°C and 24°C. A significant reduction in the power output of the Micro Gas Turbine was observed as the intake temperature was increased. The proposed case scenario caused a reduction in Nitrogen Oxide emissions in the range of 0.04 - 0.02 $g.km^{-1}$ because of the lower combustion temperature at hot intake temperature. However, Hydro Carbon and Carbon Monoxide emissions have not shown noticeable reduction during the power output degradation. The experimental results have highlighted the potential issues of using the Micro Gas Turbine at higher intake temperatures and may suggest design change to take the effect of higher engine bay temperature into account.

Keywords Micro Gas Turbine · Hybrid Vehicle · Range Extender · Test Characterization

Abbreviations

BEV	Battery Electric Vehicle
HEV	Hybrid Electric Vehicle
IC	Internal Combustion
MGT	Micro Gas Turbine
SOC	State of Charge
HC	Hydro Carbon
CO	Carbon Monoxide
NOx	Nitrogen Oxide
WLTP	Worldwide Harmonised Lightweight Test Protocol
NEDC	New European Drive Cycle
rpm	revolution per minute
AFR	Air Fuel Ratio
SFC	Specific Fuel Consumption
PTFM	Pitot Tube Flow Meter
TIT	Turbine Inlet Temperature

1 Introduction

Demand for BEV and HEV is forecast to increase significantly beyond 2020 because of several influential factors such as stricter legislation to protect the environment, government incentives, higher fuel costs and improved infrastructure for vehicle charging [1]. On-going research are focused on the enhancement of the technical aspects of BEV and HEV to attain positive customer perception and higher vehicle acceptance levels [2]. These attributes have been acknowledged as limiting factors explaining the low market demand during recent years, particularly in the BEV segment. Another disadvantage that can be associated with BEV is the typically much reduced range compared to an IC engine powered vehicle. This is mainly due to the capacity of the batteries to deliver a sufficient amount of energy [3]. Additionally, the packaging area within the vehicle available for energy storage, ancillary drive power demand and vehicle safety requirements have affected BEV range [4]. The next generation of Lithium-Ion batteries can deliver a high energy density at approximately 250 - 300 $Wh.kg^{-1}$, which gives a vehicle range of more than 200 miles per single charge for many current vehicles [5]. However, this range is dependent on the vehicle platform segment and the aggressiveness of the driving patterns [3]. The vehicle range issue associated with the battery energy density for BEVs can be resolved with the introduction of a range extender, which is used to recharge the battery pack while the vehicle is being driven, turning a BEV into a HEV.

Most of the automotive manufacturers adopt a downsized IC engine as the range extender due to its proven technology [6, 7]. It is reliable, efficient, can be designed for petrol or diesel fuel and is relatively small for ease of vehicle packaging. However, the undesired inherent features of IC engines such as noise, vibration and harshness, and exhaust tail pipe emissions issues have led to research to find alternative power sources. Fuel cells, Wankel engines and MGT have been benchmarked against the IC engine for the range extender technology [8, 9]. Previous research has highlighted six attributes of the technologies in terms of the advantages and the disadvantages such as power density exhaust tail pipe emissions, serviceability, NVH, bill of material cost and production readiness [10]. The studies show that the MGT has more potential advantages as a range extender compared to other technologies [9]. For instance, the gaseous emissions particularly CO and HC, are low for typical operating regimes (11). Additionally, due to the continuous combustion and the simplified rotating component architecture, the vibration and the harshness of the MGT is lower compared to the IC engine as well as the reduction in maintenance. The general design concept of an MGT-based range extender is typically to supply a constant power output to the high voltage bus on the vehicle, which can power the electric machine and/or recharge the vehicle battery. With this power output behaviour, it is not necessary to run the MGT based on vehicle speed or power requirement. Typically, range extender vehicles are operated based on battery SOC rather than power demand i.e. more concerned with energy provision rather than power provision. However, for reasons such as local emissions performance, battery charge acceptance and battery temperature, it may be advantageous to run the MGT at a number of power levels, and the performance of MGTs when used in this way is not well understood.

The aim of this paper is to understand the MGT performance in terms of efficiency, emissions and response to changing demands, including hot and cold start behaviour. This will be achieved through consideration of several test case studies covering the performance of the MGT for cold and hot starts, for cold and hot ambient temperatures, and for MGT response to step changes in power demands. The manuscript will include a description of the newly developed experimental methods that will allow this to be achieved. This manuscript is organized as follows. Section 2 gives a background to MGTs for range extender applications, Section 3 describes the experimental developments, Section 4 describes the results and the conclusions are described in Section 5.

2 MGT as a Range Extender in EV and HEV

In the automotive sector, several companies such as General Motors, Rovers and Nissan have attempted to use MGT as the power plant to propel the wheels directly using a step down gear ratio [12]. The works were hampered by the feeling of turbo lag at low shaft speeds due to the parasitic losses. As a result, automotive MGT development was neglected until the recent popularity of HEVs when an alternative power plant to the IC engine has been considered. In these vehicle technologies, the MGT was used in the cogeneration concept to charge the battery energy storage and to power the electric machine via an alternator. Cogeneration or Combined Heat and Power is a concept where both electrical and thermal energies are generated from the same fuel source and both type of energies are usefully used. A typical configuration of a cogeneration automotive MGT consists of a single stage turbine and a compressor connected by a shaft as described in [9].

A typical shaft speed is more than 100,000 rpm and operates at a high temperature environment between 315 °C and 370 °C. As a result, an air bearing is used that can work at both high shaft speed and high operating temperature [13]. The shaft is also connected to a generator unit, to generate a 3-phase alternating current. The most common design of MGT generator is based on the permanent magnet type due to its lower cost and simple architecture compared to other types of motors such as switch reluctance motor. An intake air is induced through the generator where it acts as a coolant, before it is compressed by the compressor unit. The air filter is used to provide a clean intake air for preventing any damage towards the rotating component, and to improve air quality for performance improvement [9]. The compressed air flows into a recuperator system, which acts as a heat exchanger, then provides an additional increase in the temperature of the compressed air. The compressed air then enters the combustion chamber, where fuel is injected and the continuous combustion process takes place. The high temperature combustion gases then turn the turbine unit and exits to the recuperator system where its heat is transferred to the incoming intake air. The fluid dynamics behaviour of the turbine is controlled by the rotor size, the distance between the compressor and the turbine; and the manufacturing tolerances of the rotor design [14]. Previous work has shown that by changing these properties, the characteristics of fluid dynamics across the turbine blade can be altered, which subsequently reduced the MGT net efficiency [15]. The efficiency, however, can be increased by using a recuperator system at the end of the gas turbine cycle. A recuperator system is implemented to increase the performance efficiency by 10 % – 15 %. Typical MGT efficiency is about 15 % compared to a full-scale gas turbine of 60 % [16]. The much cooler exhaust gas then exits the recuperator system into an exhaust system. This process increases the overall efficiency of the MGT.

The MGT architecture is relatively simple, reduces the overall weight, and hence increases the power density compared to IC engine. Of particular interest in this manuscript is the recent research work that has identified several factors that influence the behaviour of MGTs, particularly the performance output and the NOx gas emissions [9] such as intake air temperatures and air mass flow rate. The NOx formation in MGTs due to the high combustion temperature is high particularly when it reaches a stoichiometric mixture and a maximum power output regime [17].

There are also concerns with the exhaust gas temperature, the power response at cold ambient temperature and the efficiency at low power levels due to its flow dynamic behaviours. The HEV energy management system may require a power plant to respond quickly to a power demand request and at the same time to minimize the exhaust gas emissions at certain combinations of operating conditions, for example at low battery SOC.

3 Experiment Set-Up for MGT in Engine Test Cell

A black box MGT with 25 kW electrical power output (power output) at 96,000 rpm was used to investigate the highlighted concerns in a state-of-the-art vehicle engineering test facility. Due to the whole unit configuration, no access to the MGT controller and the power electronics has been given except the power demand input. The MGT was instrumented with pressure transducers (absolute pressure at 35 kPa), resistance temperature detectors (Pt100 Class A 1/3 DIN) and K-types thermocouples to measure all critical boundary conditions. All of the measuring sensors and thermos-couple were calibrated based on the supplier's technical recommendations. An automotive air intake system and an exhaust system were also mounted to the MGT to replicate vehicle operational conditions [9]. Fig.1 shows the experimental set-up of MGT with an electrical system, a controlled cell temperature, a fuel metering system and emission kits.

A calibrated Diesel fuel was supplied to the MGT through a conditioned unit fuel meter together with 5 bars filtered air to assist the atomization of fuel. The specifications of Diesel fuel is shown in Table 1. A power electronics module was connected to a battery bank, which consists of 20 unit 12 V 44 Ah lead acid batteries.

Table 1. Calibrated Diesel fuel properties

Parameters	Value	Unit
Density at 15 °C	0.8348	$g.ml^{-1}$
Cetane Number	52.3	units
Flash Point	69	°C
Viscosity at 40 °C	2.48	$mm^2.s^{-1}$
Sulfur	6.7	$mg.kg^{-1}$
Carbon Residue on 10% Dist. Residue	<0.1	% mass
Water Content	80	$mg.kg^{-1}$
Fatty Acid Methyl Ester content	4.7	$\% v.v^{-1}$
Oxygen content	0.56	$\% m.m^{-1}$
Carbon Content	86.16	$\% m.m^{-1}$
Hydrogen Content	13.28	$\% m.m^{-1}$
Gross Calorific Value, Q_{HV}	45.38	$MJ.kg^{-1}$

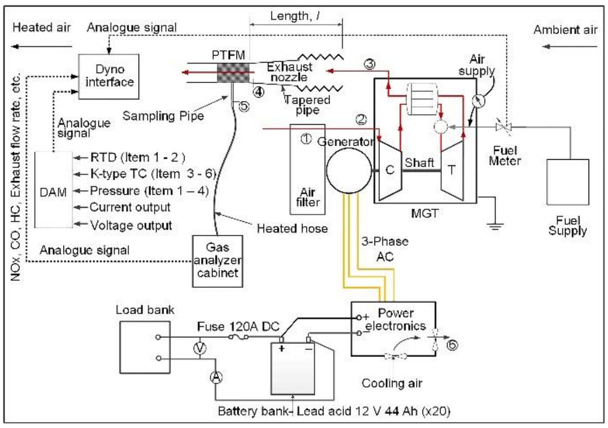

Fig.1 Range extender MGT experimental set-up using automotive sub-system components and measuring equipment

A load bank was to simulate the energy requirement of the vehicle system from the battery based on a duty cycle and to protect damage to the battery bank. Combinations of new rigs, fixtures and existing facilities were designed to follow the automotive specifications and to replicate as closely as possible potential vehicle requirements. The architecture in Fig.1 allows for better interaction within the sub-systems and providing reliable data such as power output, temperature and pressure.

The net efficiency of MGT is calculated based on the power output, the fuel mass flow rate, $\dot{m}_{fuel}$ and the fuel calorific value, Q_{HV} as shown in equation 1. The fuel mass flow rate was logged using the fuel metering system, which is yearly calibrated by the manufacturer. This method gives an overall efficiency inclusive of thermal, mechanical and electrical losses.

$$\eta_{net} = \frac{P_{output}}{\dot{m}_{fuel}\, Q_{HV}} \tag{1}$$

The power output can be obtained from the measured output voltage V_o and output current I_o that is absorbed by the load bank. Then, the net efficiency becomes

$$\eta_{net} = \frac{V_o I_o}{\dot{m}_{fuel}\, Q_{HV}} \tag{2}$$

Another important parameter that needs to be examined is the AFR. The volume flow rate of exhaust $\dot{V}_{exh}$ and the exhaust absolute pressure p_{abs} are measured by PTFM. The exhaust gas temperature T_{exh} is measured by K-type thermocouple before PTFM. These parameters will allow the exhaust mass flow rate to be calculated using the equation below.

$$\dot{m}_{exh} = \frac{(p_{atm} - p_{abs})\dot{V}_{exh}}{RT_{exh}} \tag{3}$$

Where p_{atm} is the atmospheric pressure measured by the engine test cell pressure sensor and R is the specific constant of exhaust gas. Subsequently, the AFR can be calculated:

$$\text{AFR} = \frac{\dot{m}_{exh}}{\dot{m}_{fuel}} - 1 \tag{4}$$

The ambient temperature was measured by the weather station and the intake air temperature was measured by two resistance temperature detectors that were installed in opposing direction to each other for data consistency. Then, the cell temperature and the intake air temperature were correlated so that the cell fans speed can be controlled accordingly to give the correct value of cell temperature. The exhaust gas emissions from the MGT were measured against a European Union emission regulations amended in 2004 based on Directive 70/220/EEC (Euro 6c). This work is only focused on the CO, NOx and HC+NOx values as shown in Table 2 since the Diesel fuel was used as the energy source for the MGT. The Particulate Matter was not measured because the MGT continuous combustion process produced a negligible amount of particulates. The test duration was 1800 seconds with 1 second interval based on WLTP test duration. The test was repeated two times using the same parameters setting and the test results in this paper were based on average reading for all parameters.

Table 2. European emission standard for Diesel Passenger Vehicles (Class M), g.km^{-1}

CO	NOx	HC+NOx
0.5	0.080	0.170

3.1 PTFM Sampling Pipe Length Calibration

PTFM was used to sample the exhaust tail pipe emissions to the gas analyzer through a standard pipe length. Due to the high exhaust temperature and the fast flow rate of exhaust volume of the MGT, the sampling pipe was calibrated accordingly based on the gas analyzer specifications. The sampling temperature needs to operate above the dew point temperature at 40 °C (100% relative humidity) to avoid any sample contamination with water and below 191 °C to prevent any damage to the gas analyzer unit.

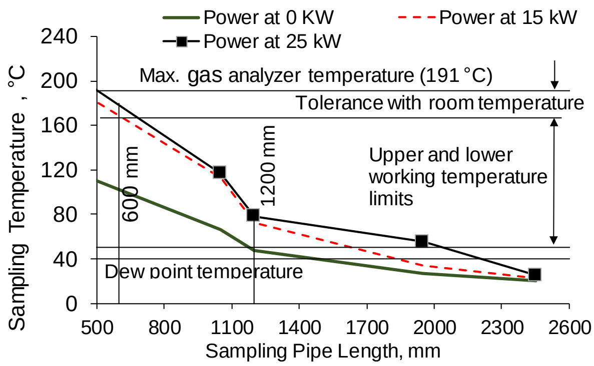

Fig.2 PTFM calibration at different pipe length and exhaust gas sampling temperature

To calibrate the sampling pipe length, the MGT was run at idle speed with approximately zero power output. Different sampling pipe lengths were used with one end was connected to the PTFM and the other end was fitted with K-type thermocouple. The temperature was recorded against the sampling pipe length for several test iterations. The processes were repeated for 15 kW and 25 kW power output. Fig.2 shows the calibration results of the sampling pipe length and the exhaust sampling gas temperature. From the test results, the recommended sampling pipe length to meet all test conditions is between 600 mm and 1200 mm.

3.2 Test Definitions and Procedures

The standard test temperature for WLTP is at 23 °C compared to 20 °C – 30 °C of that NEDC. This temperature setting was used as the benchmark to measure the characteristics of the MGT. The variation of power delivery against ambient temperature based on the black box MGT manufacturer specifications is shown in Fig.3. This relationship guides the characterization study of the MGT response and the emissions attributes. The MGT produces a constant electrical power output between -20 °C and 18 °C (*knee temperature*) before it starts to degrade because of change in air properties such as density. The net efficiency degrades in a different manner compared to the power output, which shows a close relationship with the ambient temperature.

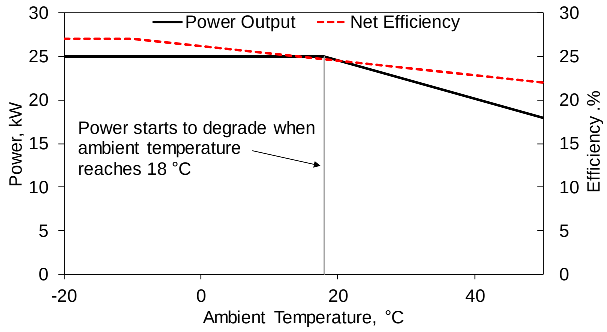

Fig.3 A black box MGT power output and net efficient specifications based on -20 °C and 50 °C ambient temperature

The effect of operating temperature on MGT performance was characterized using two test procedures, namely cold test cycle and hot test cycle. These two cycles were based on the test results performed by [9].

- Cold cycle – initial exhaust gas temperature below 50 °C.
- Hot cycle – initial exhaust gas temperature is above 50 °C.

To maintain and to define the steady-state performance of MGT, the tests were also be divided into two regimes:

- Cold - test cell temperature below 18 °C.
- Hot - test cell temperature above 18 °C

These two temperature regimes were used to reflect the performance of MGT at before and after the *knee temperature*.

Finally, the combination of these proposed test procedures were implemented to characterize the MGT for performance, exhaust tail pipe emissions and sensitivity to the intake air temperature. The two ambient temperatures and the two MGT exhaust temperatures form the test procedures in the next sections. There were two power demands proposed to excite the MGT, namely constant power demand and interval power demand as shown in Fig. 4.

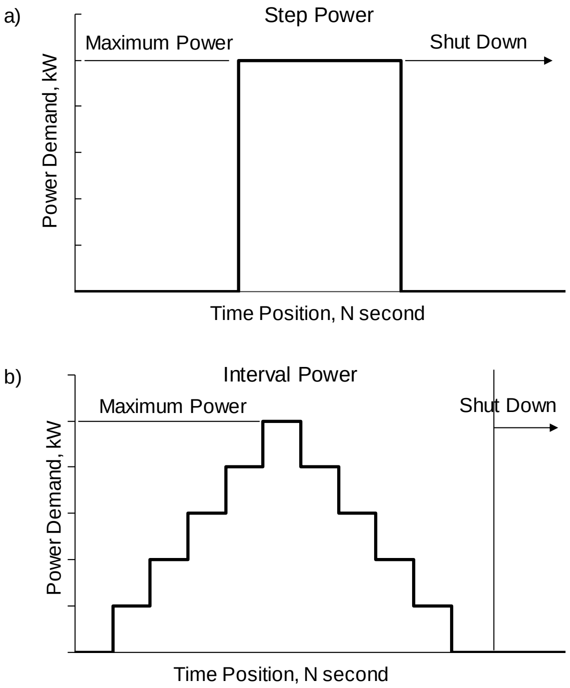

Fig.4 Step power and Interval power demands for MGT characterization studies at cold test and hot test cycles with ambient temperature below and above 18 °C for performance, gaseous and sensitivity to the intake air temperature

3.2.1 Constant Power Demand Test Method

To achieve one of the work objectives and the performance correlation, the intake air temperature was varied between 10 °C and 24 °C whilst minimizing the pressure depression value of test cell. The temperature range was to replicate the majority of MGT operating conditions. The proposed temperature range was sufficient to investigate the power degradation and the *knee temperature* characteristic. Two fans in the dynamometer cell were initially turned on with appropriate speeds for 30 minutes until the cell temperature was maintained at 10 °C based on the ambient temperature. A maximum constant power demand at 25 kW was then used to excite the MGT as shown in Fig.4(a). Subsequently, the cell temperature was increased with 2 °C interval by reducing the fans speed. This method allows for the characterization of MGT for sudden temperature change. Table 3 shows the test procedures to characterize the MGT based on two cycle temperatures and two cell temperatures.

Table 3. MGT test procedures for Step Power demands

	1st Test Procedure	2nd Test Procedure
Power Demand	Maximum Step	Maximum Step
Cycle	Hot	Cold
Cell Temperature	Cold	Hot

3.2.2 Variable Power Demands Test Methods

The power demand, as shown in Fig.4(b) was used to characterize the MGT with an interval of 5 kW. These test procedures were to allow the analysis of the transient power response and the exhaust tail pipe emissions for sudden changes in power demand at different vehicle loads. In these test conditions, the cell temperature was controlled below 18 °C with an initial temperature at 10 °C in order to have a no power output degradation throughout the test. Two cycles were used to run the MGT, namely Cold and Hot. Table 4 shows the sequence of the test operations. The 3rd test procedure was initially running until it had completed the whole process. The 4th test procedure was started when the exhaust gas temperature was still above 50 °C. These test procedures were used to investigate the characteristics of MGT at start-stop vehicle conditions.

Table 4. MGT test procedures for Variable Power demands

	3rd Test Procedure	4th Test Procedure
Power Demand	Interval	Interval
Cycle	Cold	Hot
Cell Temperature	Cold	Cold

4 Test Results and Characterization Studies

In this section, the test results will be discussed in detail on the MGT attributes such as power output, AFR, net efficiency and exhaust tail pipe emissions. Additional test that was performed to investigate the sensitivity analysis of the power output to the varying cell temperature will also be discussed.

4.1 MGT Constant Power Demand and Different Cycle and Cell Temperature Settings

4.1.1 Hot Cycle and Cold Cell Temperature

In Fig. 5, the response time of the power output to the power demand is significantly slower than a typical IC engine of similar size at 75 seconds. The MGT holds the maximum power output until it completes the WLTP time cycle. During the test period, the turbine speed was observed to maintain its maximum speed at 96,000 rpm and to keep the maximum net efficiency by inducing a maximum airflow rate. The net efficiency value is at 23 % and within the manufacturer's specification at the test temperature range. The AFR is high during start-up before it starts to stabilize at 58:1 as the power output reaches the steady state condition, which is similar to IC engine start up behaviour. The exhaust gas temperature at steady state condition is 270 °C, which is about the same as the Diesel IC engine gas tail pipe temperature [18].

When the MGT was requested to stop at the end of the test period, the power demand was set to zero with no fuel supply. The fall rate of the power output is faster than the rise rate, but requires approximately 40 seconds to reduce from the maximum power output to zero power output. The MGT is required to run in cooling off (shut down) mode to protect the system components such as the rotating shaft by using the access heat in the recuperator system to turn the turbine unit. The shut down mode takes approximately 10 minutes and the turbine was running at idle speed of 45,000 rpm. The MGT is also required 0.31 kW.h of battery energy to rotate the turbine using the generator system.

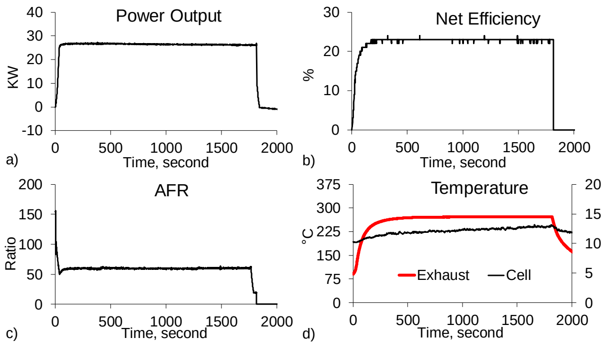

Fig.5 MGT relationships between power output, AFR, net efficiency at hot cycle/cold cell temperature

In Fig.6, the CO emission is observed peaks during start up, which is much dependent on AFR and gradually stabilize at about 0.005 g.km^{-1}. The spike seen during shut down mode is due to the purge mechanism in the atomizer that removed the excess fuel in the fuel line system. This behaviour can also be seen in other test procedures. The NOx emission level follows the same trend as CO and this is due to the access of air that increases the combustion temperature. It starts to stabilize after 130 seconds. For HC+NOx emissions, the results have been influenced by their independent behaviours through the power demand and AFR. In average, the exhaust gas emissions comply with Table 2 requirement based on WLTP time cycle when operating at steady-state maximum power output.

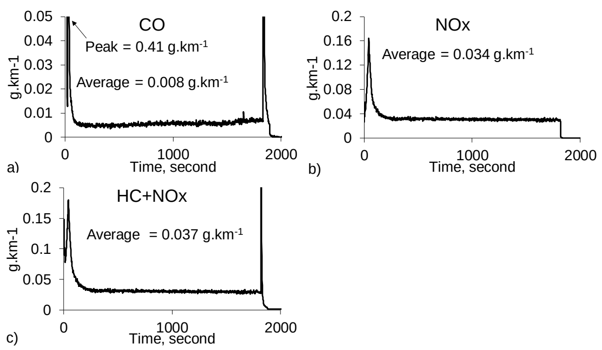

Fig.6 MGT exhaust gas emissions at maximum power output and hot cycle/cold cell temperature

4.1.2 Cold Cycle and Hot Cell Temperature

Fig.7 shows the results of 2nd test procedure for the MGT attributes. The MGT was running at an idle speed of 45,000 rpm when the maximum power was required. At this condition, the MGT efficiency was low. This is due to the low initial recuperator temperature. Hence, the TIT did not reach the optimum operating temperature. [19] study shows that the efficiency of the MGT is sensitive to the TIT. A similar sized MGT typically will require TIT between 840 °C and 900 °C [20]. More fuels were demanded to run the MGT at idle speed until it reached the exhaust gas temperature at 50 °C. From this temperature onwards, the power output started to ramp up until it reached the power demand. It took approximately 56 seconds to reach the desired exhaust gas temperature. However, the power output is observed to degrade parabolically until it reaches 21 kW when the cell temperature is 23 °C at the end of WLTP time cycle.

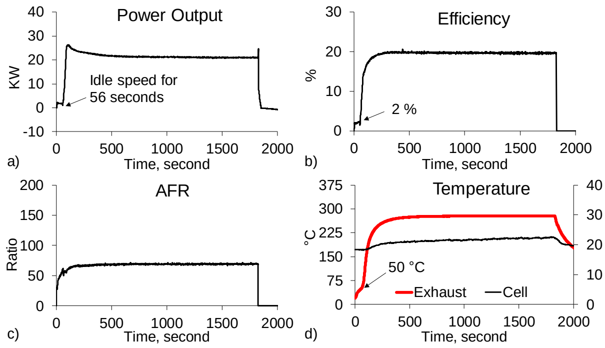

Fig.7 MGT relationships between power output, AFR, net efficiency at cold cycle/hot cell temperature

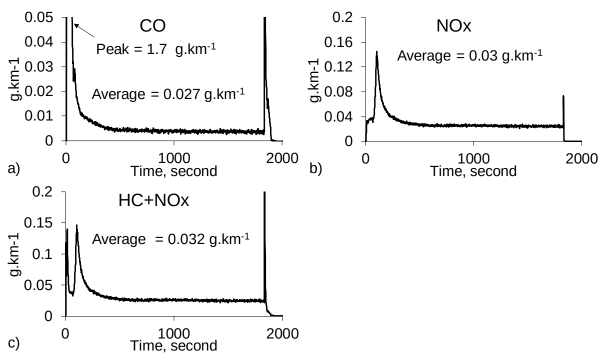

Fig.8 MGT exhaust gas emissions at maximum electrical power output and cold cycle/hot cell temperature

Based on Fig.3, the deviation with the power output in this test procedure at 23 °C is 2 kW due to several factors such as intake air quality and pressure drops in the recuperator system. The exhaust gas temperature at steady state condition is also higher than 1st test procedure at 280 °C. The power output degradation at hot cell temperatures highlights a potential issue with the energy management within the HEV, particularly concerning the engine bay thermal management requirement. During shut down mode, there is no significant change in the behaviour compared to the 1st test procedure.In Fig.8(a), an interesting observation is that the CO emission peaks were four times higher than the 1st test procedure and exists for a longer time. This is due to the lower AFR at idle speed that changes the combustion quality as can be seen in Fig.7(d), where the exhaust gas temperature rise rate is slower compared to the 1st test procedure. During idle speed, there is a low NOx level produced by the MGT. The higher cell temperature has not changed the peak of NOx emissions from the idle speed power output to the maximum power output and at steady state condition as the exhaust gas temperature is not significantly different. In term of the HC+ NOx emission, other than the influence of higher AFR during initial start up, the combined emission is dominated by the NOx behaviour. In summary, the average exhaust gas emission still meets Table 2 requirement even though the CO emissions is three times higher than 1st test procedure due the above explanations.

4.2 MGT Variable Power Demand and Different Cycle and Cold Temperature Settings

The behaviours of MGT based on 3rd and 4th test procedures are shown in Fig. 9. When there is no power demand, the MGT is running at idle speed and generates approximately 1.5 kW of power output. At idle speed condition, both cycles show no significant differences in term of power output. For both incremental and decremental step changes in the power demand, the MGT is able to respond within 40 seconds. The power outputs can meet the demands at every level apart from the maximum demand, which also corresponds to the maximum test cell temperature. Similarly, when the power output is at maximum, it starts to decrease by approximately 5 % for both cycles.

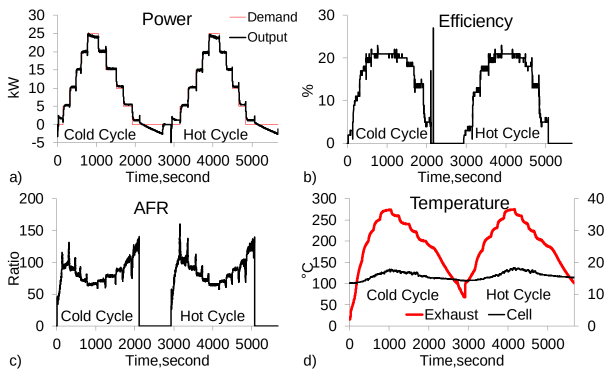

Fig.9 MGT relationships between electrical power output, AFR, net efficiency at cold cycle/hot cycle and cold cell temperature

In both test procedures, the CO emission spikes during initial start-up and starts to reduce when more power is demanded with a richer mixture as shown in see Fig.10(a). Generally, the NOx emission increases as the power demand is increased because of higher combustion temperature at higher power output. Interestingly there are small NOx peaks during both hot and cold operations when a power reduction is made. In term of the HC+ NOx emission, other than the influence of higher AFR during initial start-up, the combined emission is dominated by the NOx behaviour.

A trade off approach was used to understand the optimum power demand that includes the net efficiency, the SFC and the NOx emission (see Fig. 11). Both 20 kW and 25 kW power outputs produced similar levels of efficiency at 21 % with an average SFC of 408 $g.kW^{-1}.h^{-1}$ and 398 $g.kW^{-1}.h^{-1}$ respectively. The similar efficiencies are due to the linear relation between the compressor pressure ratio and the TIT at both power outputs. However, the NOx emissions are much lower at 20 kW compared to 25 kW (0.025 $g.km^{-1}$ and 0.045 $g.km^{-1}$ respectively) which means that if there are concerns over the NOx emissions in the final application, then the preferred MGT operating point may be at 80 % of the power output rather than maximum output. From all tests performed above, it is acknowledged that the *knee temperature* has changed and influenced the performance of the MGT at maximum power output.

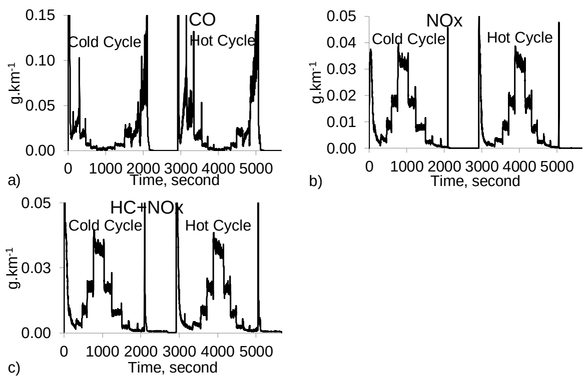

Fig.10 MGT exhaust gas emissions at maximum electrical power output at cold cycle/hot cycle and cold cell temperature

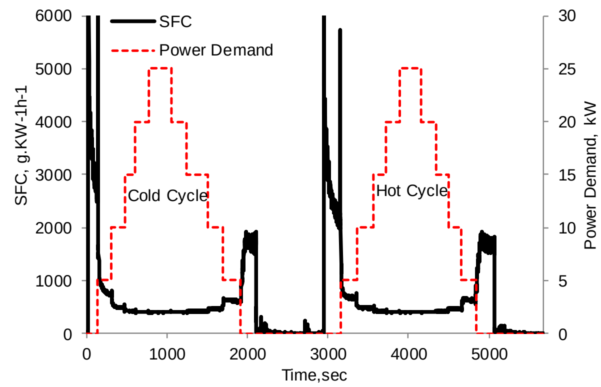

Fig.11 MGT SFC trade-off for interval step power demand at cold cycle/hot cycle and cold cell temperature

It is important to understand the sensitivity of the ambient temperature in relation to Fig. 3. Another test was performed with different parameters setting. The power demand was set at maximum (25 kW) and the cell temperature was varied between 12 °C and 24 °C with 2 °C temperature interval using cold cycle condition. Fig.12(a) shows the results based on the test condition where the power output and the cell temperature have been normalized using the equation 5 between the cell temperature 12 °C and 24 °C.

$$\text{Data}_{normalized} = \frac{abs(\text{Data}_{a} - \text{Data}_{n+a})}{\max(\text{Data}_{a \to n+a})} \quad (5)$$

From Fig.12(b), the ratio of both normalized data shows a linear relationship of the cell temperature. The nonlinear behaviour when the cell temperature is abruptly reduced shows that the MGT is sensitive in a sudden change of intake air temperature.

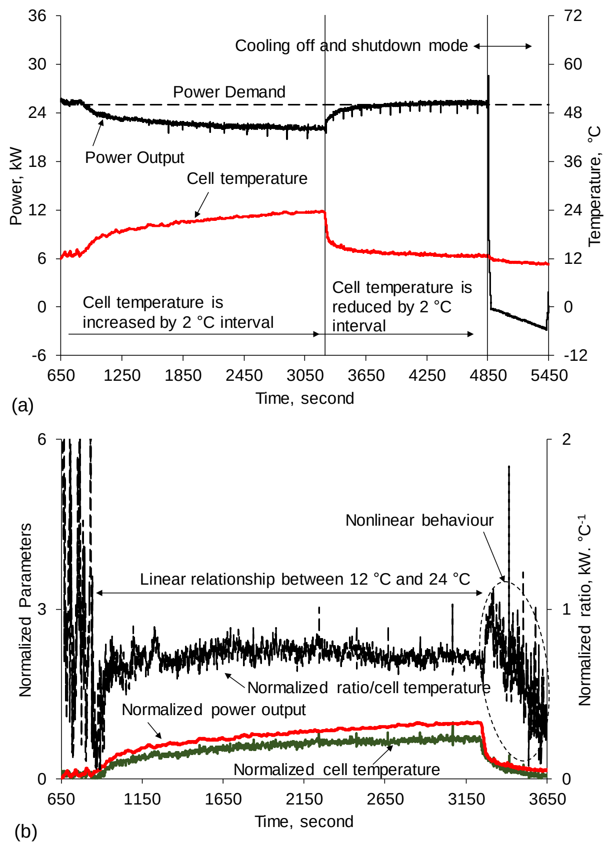

Fig.12 MGT relationships at cell temperatures between 12 °C and 24 °C at constant power demand and maximum shaft speed a) Power output vs. cell temperature b) Normalized power output vs. normalized cell temperature

Figure 13(a) shows the correlation of power output from the MGT specification and the test data. The *knee temperature* is reduced from 18 °C to 14 °C. As a result, the power output at the standard *knee temperature* is reduced by approximately 2 kW. There are several potential reasons for this power output behaviour such as:

- Compressor or Turbine fouls change air aerodynamics
- Quality of intake air change its properties
- Recuperator leaks reduce its thermal efficiency.

The reduction rate of power output is 0.2 kW for every 1°C cell temperature increase, the same reduction rate as per specification beyond the *knee temperature*. The consequence of the power output behaviour may give an implication to the HEV energy management strategies. This is because the WLTP automotive test standard operates at 23 °C, where the loss of power output can change the vehicle speed profile and the batteries SOC.

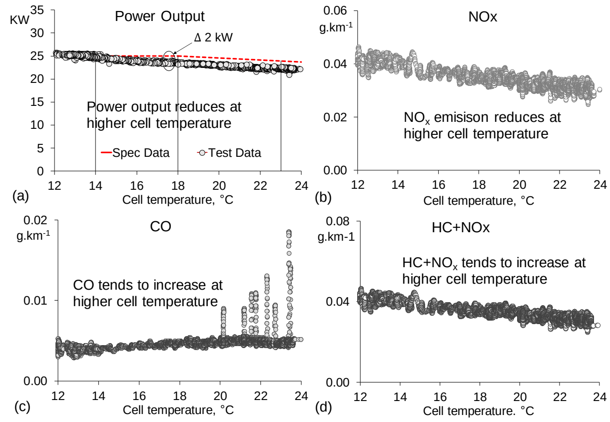

Fig.13 MGT relationships at cell temperatures between 12 °C and 24 °C at constant power demand and maximum shaft speed with a) Power output b) NOx emission c) CO emission d) HC +NOx emission

5 Conclusions

The black box MGT has been successfully tested using an automotive test facility for different operating conditions. These approaches have introduced new validation techniques for MGTs within automotive test requirements when used as a range extender. It has been acknowledged that the response time in term of power output for the MGT is significantly longer than the response time of IC engines. This issue leads to the requirement for further research into the energy management strategies of vehicle, particularly the MGT responses during steady state and transient power demands at cold conditions.

The new techniques in these studies have been implemented successfully to investigate the sensitivity of MGT to the cell temperature. Several findings have been highlighted to understand the implication of temperature variation to the MGT in the automotive application such as:

- Linear power output reduction at *knee temperature* 14 °C instead of 18 °C.
- Power output is responsive to the sudden cell temperature change
- Net efficiency also drops and varies to the temperature change

These findings require further detail studies of vehicle packaging for MGT as a range extender in order to prevent any power output surges, particularly at extreme hot conditions and are not eliminating the range anxiety issue for HEVs. One of the solutions for this concern is to have a better air flow circulation within the engine bay using a bigger radiator fans or a water-cooled air intake system. Another design approach is to oversize the MGT. However, the approaches need to know the vehicle energy requirement and the impact of oversizing the MGT to the vehicle system. For instance, the additional weight can increase the overall energy consumption of the vehicle.

The battery power output is significantly reduced at very low temperatures i.e. < 0 °C. If the battery SOC is low at this temperature condition, the delay in responding to the vehicle power demand cause some major concerns in terms of performance attributes and safety. New energy management strategies need to be investigated to overcome these potential issues.

In term of the exhaust tail pipe emissions, much higher AFR and fuel consumption compared to IC engine has not increased the level of emissions. The test results show that the MGT is compliant to Euro 6c emissions at various test conditions. In fact, the low amount of emissions that the MGT produces require no exhaust after treatment, hence ease the vehicle packaging and reduces the overall component cost. The sensitivity analysis on the exhaust tail pipe emission such as CO, NOx and HC+NOx emissions are proportional to the cell temperature. Even though the predicted level of exhaust tail pipe emissions at the upper and lower end of the operating temperature is still within the Euro 6 limits, an advanced passive thermal management system is desirable as suggested above.

In summary, the MGT potentially can be adapted as a range extender in HEV if the power output reduction at higher cell temperature can be minimized to cope with the vehicle energy and the vehicle system requirements**.** Additionally, more work is also needed to be carried out to investigate more aggressive power demand at cold and hot ambient conditions i.e. -40 °C and 50 °C for providing robust energy solutions to HEVs.

Compliance with Ethical Standards

Conflict of interest On behalf of all the authors, the corresponding author states that there is no conflict of interest.

References

1. Global EV Outlook 2019, IEA, Paris https://www.iea.org/reports/global-ev-outlook-2019 (2019). Accessed 25 February 2020
2. Electric vehicle in Europe: gearing up for a new phase?, Amsterdam Roundtable Foundations and McKinsey & Company, The Netherlands (2014). Accessed 24 February 2020
3. Varga, B.O., Sagoian, A., Mariasiu, F.: Prediction of Electric Vehicle Range: A Comprehensive Review of Current Issues and Challenges. Energies. 12, 946 (2019). https://doi.org/10.3390/en12050946
4. Turner, J., Blake, D., Moore, J., Burke, P. et al.: The Lotus Range Extender Engine. SAE Int. J. Engines 3(2):318-351 (2010). https://doi.org/10.4271/2010-01-2208
5. Li, J., Du, Z., Ruther, R.E. et al.: Toward Low-Cost, High-Energy Density, and High-Power Density Lithium-Ion Batteries. JOM 69, 1484–1496 (2017). https://doi.org/10.1007/s11837-017-2404-9
6. Cooper, A., Stodart, A., Hancock, D., Duke, S. et al.: Development of Two New High Specific Output 3 Cylinder Engines for the Global Market with Capacities of 1.2l and 1.5l. SAE Technical Paper 2019-01-1193 (2019) doi:10.4271/2019-01-1193
7. Nieuwenhuis, P., Cipcigan, L., Berkem, :The Electric Vehicle Revolution, In Future Energy, pp. 227-243. Elsevier (2020)
8. Smallbone, A., Jia, B., Atkins, J., l Roskilly, A.P.: The impact of disruptive powertrain technologies on energy consumption and carbon dioxide emissions from heavy-duty vehicles, Energy Conversion and Management: X, Volume 6 (2020), https://doi.org/10.1016/j.ecmx.2020.10003
9. Shah, R.M.A., McGordon, A., Amor-Segan, M., Jennings, P.: Micro gas turbine range extender-Validation techniques for automotive applications. Paper presented at IET Hybrid and Electric Vehicles Conference 2013 (HEVC 2013), 6–7 November 2013
10. Klostermann, A.: Trends and developments in range extender technology. Proceedings of the FISITA 2012 World Automotive Congress: Volume 3: Future Automotive Powertrain (1), (2012)
11. KarvountzisKontakiotis,A.,Andwari,A.M.,Pesyridis,A.,Russo,S.,Tuccillo,R.,Esfahanian, V.: Application of Micro Gas Turbine in Range-Extended Electric Vehicles, Energy, Volume 147 (2018) https://doi.org/10.1016/j.energy.2018.01.051
12. Ohkubo, Y.: Outlook on Gas Turbine. R&D Review of Toyota CRDL, 41(1) (2005)
13. Shan, X.,Zhang, Q.,Sun, Y., & Maeda, R.: Studies on a micro turbine device with both journal- and thrust-air bearings. Microsystem Technologies. 13. 1501-1508 (2007) https://doi.org/10.1007/s00542-006-0346-11
14. Nascimento, M.A.R.D., Eraldo, C.D.S., Gomes, E.E.B., Dias, F.L.G., Velásques, E.I.G., Carrillo, R.A.M.: Micro Gas Turbine Engine: A Review, InTech (2013)
15. Clay, A.,Tansley, G. D.: A micro gas turbine for UK domestic combined heat and power. Proceedings of the Institution of Mechanical Engineers, Part A: Journal of Power and Energy, 224(6), 839–849 (2010) https://doi.org/10.1243/09576509JPE996

16. Rena,P.G.,Kumar,S.:Chapter 6 - Landfill Gas as an Energy Source, Current Developments in Biotechnology and Bioengineering, Elsevier, p93-117 (2019) https://doi.org/10.1016/B978-0-444-64083-3.00006-3
17. Cohen,G.R.H, Saravanamuttoo, H.I.H.: Gas Turbine Theory, 4th ed., Longman, Essex, England, (1996)
18. Basaran,H.U., Ozsoysal,O.A.:Effects of application of variable valve timing on the exhaust gas temperature improvement in a low-loaded diesel engine, Applied Thermal Engineering, Volume 122, p758-767, (2017) https://doi.org/10.1016/j.applthermaleng.2017.04.098.
19. Ibrahim, T., Rahman, M.: Parametric study of a two-shaft gas turbine cycle model of power plant. IOP Conference Series: Materials Science and Engineering, 36, p.012024 (2012)
20. Gimelli, A., Sannino, R.: Thermodynamic model validation of Capstone C30 micro gas turbine. Energy Procedia, Volume 126, p655-692 (2017) https://doi.org/10.1016/j.egypro.2017.08.184